



Removal of Cu(II) from aqueous solutions using modified sewage sludge ash

S. Kul¹

Received: 29 September 2020 / Revised: 20 April 2021 / Accepted: 28 May 2021 / Published online: 7 June 2021
© Islamic Azad University (IAU) 2021

Abstract

The study aims to determine Cu(II) adsorption from wastewater in the laboratory condition using modified sewage sludge ash as adsorbent which was obtained from a thermal drying and incineration facility. This procedure was completed with an inexpensive pollutant material which has high metal-binding capacity and is available in abundant amounts. During experiments, the effects of particle size, pH, stirring speed, initial ion concentration, adsorbent dosage and temperature were investigated. Adsorption equilibrium was obtained in 10 min. Maximum Cu(II) removal was calculated as 83.63% with 20 mg L⁻¹ initial Cu(II) ion concentration and 5 g L⁻¹ adsorbent dosage. Kolmogorov–Smirnov normality test was performed to test the conformity of the data obtained as a result of the study to variance analysis, and it was determined that the data were distributed normally ($p > 0.05$). Levene test was performed for homogeneity test, and it was determined that the data were distributed homogeneously ($p > 0.05$). Langmuir was determined as the most suitable isotherm model for Cu(II) adsorption. Adsorption kinetics abided by the pseudo-second-order model. Based on kinetic studies, the adsorption process was endothermic with maximum adsorption capacity calculated as 7.53 mg g⁻¹. The results of thermodynamic research showed the adsorption reaction was spontaneous ($\Delta G^\circ < 0$), endothermic ($\Delta H^\circ > 0$) and reversible ($\Delta S^\circ > 0$ and close to zero).

Keywords Adsorption · Isotherm models · Cu(II) removal · Sewage sludge ash · Langmuir isotherm

Introduction

Heavy metals are among the important topics of recent years because of their pollution. These heavy metals, which are found in very small concentrations in nature, cause serious harm to animals, plants and people. Heavy metals such as copper, nickel, cadmium, lead and chromium need to be removed from wastewater due to their frequent occurrence in wastewater discharged from many sectors such as electroplating, metallurgy, tanning, chemical manufacturing, mining and battery manufacturing (Potgieter et al. 2006; Bingul et al. 2016; Gupta et al. 2017; Abdullahi et al. 2020). Heavy metals are often found not only in industrial wastewater but also in receiving areas such as soils and seas and

being a high risk to the environment. Moreover, they cause adverse effects on the receiving areas due to their presence with increased discharge amounts and toxicity (Dundar et al. 2008; Turan et al. 2020; Nuhoğlu et al. 2021).

Among these toxic metals, Cu is a basic micronutrient required at low levels by living organisms. However, it is toxic when found above a certain tolerance level in organisms and as a result becomes a worrying pollutant for environmental and public health. In particular, Cu mining produces large amounts of acid drainage and pollutes water sources with Cu and other heavy metals. The use of this water for agricultural activities causes accumulation of heavy metals in soils and transports from polluted soil into food (Lee 2006; Pandey et al. 2007; Tong et al. 2011). In potable water, the limit value for Cu is 2 mg L⁻¹ according to the World Health Organization (WHO), while it was determined as 1 mg L⁻¹ by the USA Environmental Protection Agency (EPA). There is a need for a variety of treatment processes to reduce the effects of copper on the environment and human health.

There are many alternative treatment processes to remove available copper ions from aqueous media including

Editorial responsibility: Fatih ŞEN.

✉ S. Kul
sinankul@bayburt.edu.tr

¹ Faculty of Applied Sciences, Department of Emergency Aid and Disaster Management, Bayburt University, 69000 Bayburt, Turkey



electrocoagulation (Escobar et al. 2006; Akbal and Camcı, 2011; Mateen et al. 2020), reverse osmosis (Rodrigues Pires da Silva et al. 2016), filtration (Aziz et al. 2001), membranes (Qdais and Moussa 2004; Kocherginsky and Yang 2007; Mojdehi et al. 2019), electro dialysis (Mohammadi et al. 2005), biochemical treatment (Zhang et al. 2012), adsorption/biosorption (Pan et al. 2003; Uoginté et al. 2019), etc.

The adsorption process used for removal of heavy metals from wastewater is a method with appropriate cost that is competitive and efficient. Heavy metals are removed from aqueous media with the aid of adsorbents. In recent times, many studies have been performed about Cu(II) adsorption with adsorbents. These studies investigated the effects of different adsorbents on Cu(II) removal, and these adsorbents may be listed as Fe₃O₄ magnetic nanoparticles (Chang and Chen 2005; Ozmen et al. 2010), sawdust from meranti wood (Ahmad et al. 2009), modified sawdust cellulose (Ulfa et al. 2019), bentonite (Bereket et al. 1997; Kubilay et al. 2007), cotton balls (Ozsoy and Kumbur 2006), fish bones (Kizilkaya et al. 2010), pumice (Turan et al. 2011), pistachio shell (Banerjee et al. 2019), herbaceous peat (Gündoğan et al. 2004), PANI-clay hybrid material (Soltani et al. 2019), etc.

In this research, the potential use of ash obtained from GASKİ Wastewater Sewage Sludge Thermal Drying and Incineration Facility (Gaziantep/Turkey) as adsorbent for the removal of Cu(II) ions was investigated. Sewage sludge ash (SSA) is the final product from the GASKİ Wastewater Sewage Sludge Thermal Drying and Incineration Facility, and though an environmental pollutant, no cost is involved. In other words, procedures which remove a waste that is harmful if discharged to the environment by using a waste which is harmful if discharged to the environment gain importance as an environmentally friendly technology. This study was carried out at the Department of Environmental Engineering laboratories of Atatürk University, and it was completed at the end of 2019. This study aimed to determine the effects of pH, initial metal ion and initial adsorbent concentration, stirring speed, temperature and particle size parameters on adsorption. Kolmogorov–Smirnov normality test was performed to test the conformity of the data obtained as a result of the study to variance analysis, and Levene test was performed for homogeneity test. Adsorption isotherms, adsorption kinetics and thermodynamic studies were also evaluated.

Material and methods

Adsorbent

The adsorbent used in the trials was SSA obtained from GASKİ Wastewater Sewage Sludge Thermal Drying and Incineration Facility located within Gaziantep provincial

boundaries. The physical and chemical properties of SSA are given in Table 1.

Before experiments, as the pH value of solutions used in raw SSA experiments continuously increased, it was washed with acid. This process ensured removal of other soluble materials from the adsorbent. Firstly, 200 g raw SSA was added to 4 L distilled water and mixed as the solution pH rose and became fixed. When the pH value stabilized, 3 mL H₂SO₄ was added. This process cycle continued at room temperature until the pH value stabilized around 4. Finally, SSA was washed with distilled water and the clean SSA which did not cause a change in solution pH values was left to dry at room temperature for several days. Later SSA was dried at 80 °C for 48 h and powdered with a powerful grinder. At the end of this process, adsorbents with particle sizes of < 0.045 mm, 0.045–0.18 mm, 0.18–0.2 mm and 0.2–0.5 mm were obtained using a vibrating sieve. The dose of adsorbent varied within the range of 1–5 g L⁻¹.

Preparation and analysis of Cu(II) ion solutions

Experiments used solutions with concentrations of 10, 20, 30, 40 and 50 mg L⁻¹ prepared with the aid of a stock Cu(II) solution with 1000 mg L⁻¹ concentration obtained commercially (Merck, Germany). Stock Cu(II) solution was prepared from CuSO₄ with analytical purity. The initial value of this solution was 4.5. H₂SO₄ and NaOH were used to set initial pH (Merck, Germany). For identification of the Cu(II) ion concentrations in solutions, a Shimadzu AA 6200 brand model atomic absorption spectrometer was used (Shimadzu, Japan).

Table 1 Some physical and chemical properties of SSA

Parameter	Unit	Value
Calorific value	kJ kg ⁻¹	< 1647
Humidity	%	< 3.58
Chlorine (Cl ⁻)	mg L ⁻¹	21.7
Fluorine (F ⁻)	mg L ⁻¹	0.4
Sulfate (SO ₄ ⁼)	mg L ⁻¹	1858
Dissolved organic carbon	mg L ⁻¹	1.2
Total soluble matter	mg L ⁻¹	5140
Total organic carbon	%	0.5
Specific surface area	m ² kg ⁻¹	449.9
Dv (10)	µm	6.24
Dv (50)	µm	45.3
Dv (90)	µm	294
Uniformity	–	1.787

Batch adsorption experiments

Batch adsorption experiments were performed with 250-mL volume Erlenmeyers by using 100 mL volume containing different concentrations of Cu(II). The effects of different initial parameters like particle size, pH, stirring speed, Cu(II) concentration, adsorbent dosage and temperature were investigated. Each experiment was performed with two repetitions to check calculations.

In order to ensure the adsorption process reached equilibrium and to prevent precipitation of adsorbent, 100 mL solutions were mixed at 100, 200, 300 and 400 rpm for 60 min. Samples (1 mL) were taken at definite time intervals (10, 20, 30, 45 and 60 min) for residual Cu(II) ions in solution. After experiments, samples were strained with filter paper and then atomic adsorption spectrophotometry was used to identify the Cu(II) concentration remaining in the medium. Removal efficiency, isotherms and other kinetic constants were calculated with the aid of the obtained results. In the study, which aimed to eliminate Cu(II) from aqueous solutions using purification sludge ash, the experiments were carried out according to the factorial trial plan. Kolmogorov–Smirnov normality test was performed using IBM SPSS Statistics 20 program to test the conformity of the data obtained as a result of the study to variance analysis, and it was determined that the data were distributed normally ($p > 0.05$). Levene test was performed for homogeneity test, another method to test its suitability for variance analysis; it was determined that the data were distributed homogeneously ($p > 0.05$). Additionally, adsorbent properties of adsorbents held on filter paper were determined with SEM, FTIR and XRD analyses.

SEM, FTIR and XRD analyses

SEM images were obtained using an FEI brand, Nova Nano SEM 450, USA device. All samples were glued to the sample stub and covered with a 10-nm gold–palladium layer. FTIR analyses of SSA used a Fourier transform infrared spectrometry device in an attempt to characterize the bonds between molecules or compounds in the structure and functional groups. A Bruker D8 Discover XRD device was used to determine the structural features of SSA before and after the experiments.

Results and discussion

In this study, the effects of particulate size, pH, stirring speed, initial metal ion concentration, adsorbent dosage and temperature were investigated for Cu(II) adsorption on

the readily available waste material of SSA. The research results including kinetic and thermodynamic outcomes are listed below.

Effect of particulate size on Cu(II) removal

Batch adsorption studies were completed with four different size intervals for SSA of < 0.045 mm, 0.045–0.18 mm, 0.18–0.2 mm and 0.2–0.5 mm. With natural pH value of the adsorbent of 3.5, these studies had initial Cu(II) concentration fixed at 20 mg L^{-1} and initial adsorbent dosage set to 2 g L^{-1} . Later experiments were performed at nearly 20°C and 200 rpm, and samples were taken at a variety of intervals during the 60-min contact duration. Data are shown in Fig. 1a.

As can be seen from Fig. 1a, when data obtained at the end of 60-min experiments are investigated, the adsorption efficiency percentage reduced with the increase in particle size. When particle size is set to < 0.045 mm, removal efficiency was 54.89%. When particle size was set to 0.045–0.18 mm, removal efficiency reduced by 7.41% to reach 47.48%, while with particle size from 0.18 to 0.2 mm, there was a 10.73% reduction to 44.16% efficiency. As can be seen from the result, the factor causing this situation is the decrease in surface area. The adsorption efficiency increases in direct proportion to the increase in total surface area (Kul et al. 2016). Batch adsorption studies in which the effect of particle size was examined were performed according to factorial trial pattern, and variance analysis determined that there was a difference between the groups ($p < 0.05$). As a result of the variance analysis, it was determined that the best removal efficiency was obtained at < 0.045 mm. Although the removal efficiency of < 0.045 mm was higher than 0.045–0.18 mm, the next studies were continued with a particle size of 0.045–0.18 mm since it would be difficult to separate adsorbents with a particle diameter of < 0.045 mm from water.

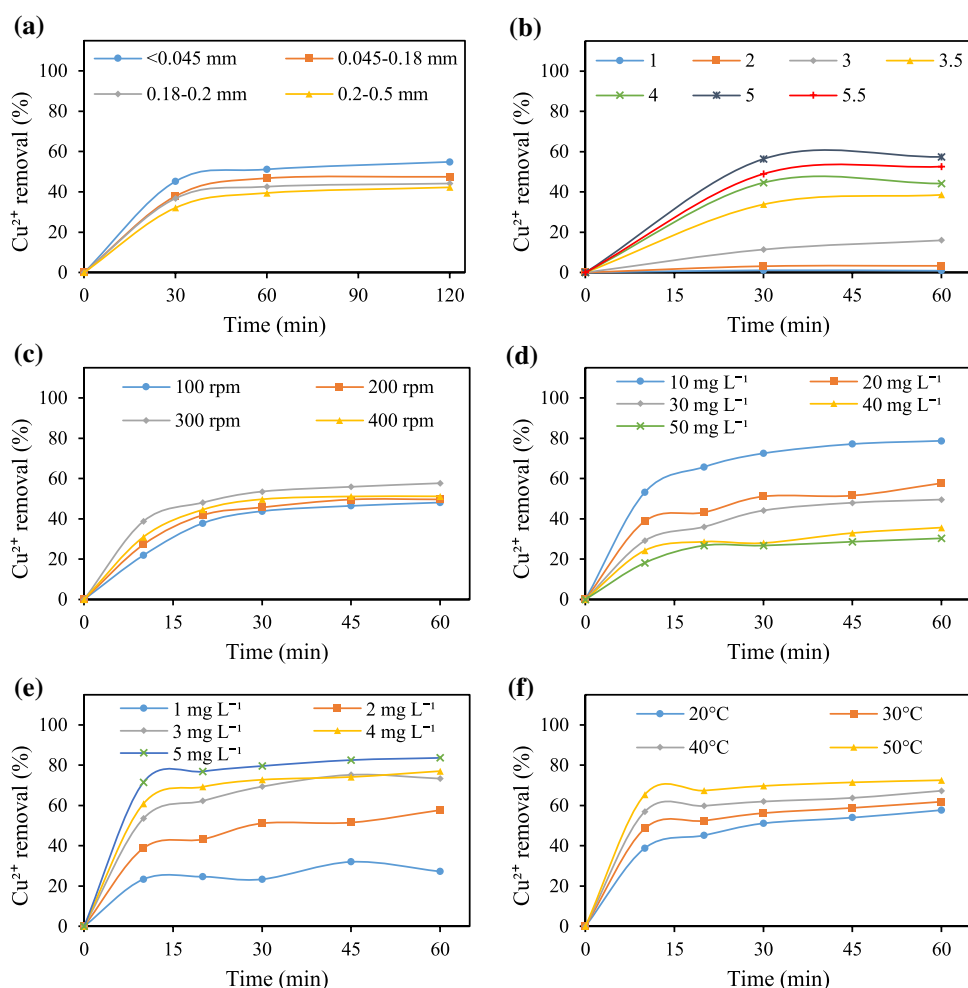
Effect of initial pH on Cu(II) removal

Studies planned for adsorption of Cu(II) ions with SSA waste material had initial pH values set to 1, 2, 3, 3.5, 4, 5 and 5.5. The initial Cu(II) concentration and adsorbent dosage values were 20 mg L^{-1} and 2 g L^{-1} , respectively, and adsorbent with diameter from 0.045 to 0.18 mm was used in experiments completed at 20°C . Experiments over 60 min at 200 rpm stirring speed had samples taken at specific times, and the Cu(II) values are shown in Fig. 1b.

When Fig. 1b is investigated, the Cu(II) removal efficiency occurred at very low rates like 0.89% and 3.31% when the pH value was set to 1 and 2, respectively. When the pH value rose to 5, there was a directly proportional increase in removal efficiency and this value was 57.39% at



Fig. 1 Effect of variation in initial parameters on the adsorption process. **a** Effect of particulate size (pH: 3.5, stirring speed: 200 rpm, C_o : 20 mg L⁻¹, m : 2 g L⁻¹, T : 20 °C), **b** effect of pH (particle size: 0.045–0.18 mm, stirring speed: 200 rpm, C_o : 20 mg L⁻¹, m : 2 g L⁻¹, T : 20 °C), **c** effect of stirring speed (particle size: 0.045–0.18 mm, pH: 5, C_o : 20 mg L⁻¹, m : 2 g L⁻¹, T : 20 °C), **d** effect of initial ion concentration (particle size: 0.045–0.18 mm, pH: 5, stirring speed: 300 rpm, m : 2 g L⁻¹, T : 20 °C), **e** effect of adsorbent dosage (particle size: 0.045–0.18 mm, pH: 5, stirring speed: 300 rpm, C_o : 20 mg L⁻¹, T : 20 °C), **f** effect of temperature (particle size: 0.045–0.18 mm, pH: 5, stirring speed: 300 rpm, C_o : 20 mg L⁻¹, m : 2 g L⁻¹)



pH 5. When the pH value is set to 5.5, the removal efficiency displayed a very slight reduction and removal efficiency was 52.57%. Due to the interaction between heavy metal hydrolysis, redox reactions and precipitation, changes in solution pH may affect adsorption (Dundar et al. 2008; Miretzky and Cirelli 2010). When the results are investigated, initial pH value appears to be one of the main factors affecting the adsorption process. The increase in adsorption capacities with an increase in pH can be explained by availability of negatively charged groups at the adsorbent surface which is necessary for the sorption of Cu(II) ions to proceed. At low pH values, Cu(II) ion removal is decreased. Surface charge becomes positive and adsorption is retarded due to competition between Cu(II) ions and H⁺ ions for the same sites (Kul et al. 2016). The highest value of removal efficiency was found as 57.39% at pH 5. In addition, in the experiments where pH changes were examined, the adsorption capacity value was calculated as 6.139 mg g⁻¹. It was decided that the pH value should be adjusted to 5 in the experiments where the effect of stirring speed will be examined, since the removal efficiency and the adsorption capacity are higher than the other pH values. In addition, as a result of

variance analysis according to factorial trial pattern, it was determined that there was a difference between the groups ($p < 0.05$), and as a result of the variance analysis, it was determined statistically that there was the best yield at pH 5.

Effect of stirring speed on Cu(II) removal

The stirrer used for batch adsorption studies was set to 100, 200, 300 and 400 rpm to investigate the effect of four different stirring speeds. Experiments using adsorbent with diameter 0.045–0.18 mm had pH value 5, initial Cu(II) concentration 20 mg L⁻¹ and initial adsorbent dosage of 2 g L⁻¹. Experiments were performed with four different stirring speeds at nearly 20 °C, and samples were taken at a variety of intervals during the 60-min contact duration. Data are shown in Fig. 1c.

When Fig. 1c is investigated, the Cu(II) removal was 48.1% when stirring speed was set to 100 rpm, while removal efficiency was 49.66% when the stirring speed increased to 200 rpm. When the stirring speed reached 300 rpm, the Cu(II) removal was maximized and occurred at 57.69% efficiency. Until this point, the removal efficiencies

of the adsorption process increased in direct proportion to the speed, but when the stirring speed was set to 400 rpm, the removal efficiency fell to 51.16%. Generally, as the stirring speed increased, contact between Cu(II) and the adsorbent surface was easier so the adsorption capacity increased. However, above a certain stirring speed, the Cu(II) ions were prevented from attaching to the adsorbent surface and this caused a reduction in removal efficiency. In other words, pore diffusion increases due to the reduction in fluid film diffusion with increasing stirring speed and increased centrifugal force (Nuhoglu et al. 2021). In the experiments where the effect of stirring speed was examined, the adsorption capacities at 100 rpm, 200 rpm, 300 rpm and 400 rpm stirring speeds were calculated as 4.82 mg g⁻¹, 4.82 mg g⁻¹, 5.94 mg g⁻¹ and 5.00 mg g⁻¹, respectively. The stirring speed was decided to be 300 rpm in the next studies, due to the fact that adsorption capacities and Cu(II) removal efficiencies were at the highest level. Moreover, the batch adsorption studies in which the effect of the stirring speed was examined were based on the factorial trial pattern and variance analysis determined that there was a difference between the groups ($p < 0.05$). As a result of the variance analysis, it was statistically determined that the best yield occurred at a mixing rate of 300 rpm.

Effect of initial Cu(II) concentration on the adsorption process

In studies to investigate initial Cu(II) concentrations, the Cu(II) concentrations were set to 10, 20, 30, 40 and 50 mg L⁻¹. Particulate size and initial pH values were 0.045–0.18 mm and 5, with studies completed using 300 rpm stirring speed, at nearly 20 °C temperature and by adding 2 g L⁻¹ adsorbent to the medium. Results are shown in Fig. 1d.

When Fig. 1d is investigated in detail, when the initial Cu(II) concentration is set to 10 mg L⁻¹ the removal efficiency was 78.73%, while increasing the initial Cu(II) concentration to 20 increased efficiency to 57.69%; at 30 mg L⁻¹ it was 49.59%; and at 40 mg L⁻¹ it was 35.67%. When the final initial Cu(II) concentration rose to 50 mg L⁻¹, the removal efficiency fell to 30.33%. Though it appears that as the initial Cu(II) concentration increases the removal efficiencies fall, the concentration of Cu(II) held per unit adsorbent was 3.92, 5.94, 8.21, 7.29 and 7.82 mg g⁻¹ with initial concentrations of 10, 20, 30, 40 and 50 mg L⁻¹, respectively. When the results of these calculated data are assessed, as initial Cu(II) concentration increases, the Cu(II) concentration held on the adsorbent surface increases to a point and remains fixed after the binding sites on the adsorbent surface are saturated (Kul et al. 2016). Removal efficiencies for the initial concentration of 10 mg L⁻¹ and 20 mg L⁻¹ were 78.73% and 57.69%, respectively. As a result of variance analysis according to

factorial trial pattern, it was determined that there was a difference between the groups ($p < 0.05$), and as a result of the variance analysis, it was statistically determined that the best yield was in the concentration of 10 mg L⁻¹. Although the removal efficiency appears to be high at the initial concentration of 10 mg L⁻¹, the adsorption capacity was 3.92 mg g⁻¹ for 10 mg L⁻¹, while it was 5.94 mg g⁻¹ for 20 mg L⁻¹. Therefore, the initial Cu(II) ion concentration was decided to be 20 mg L⁻¹.

Effect of adsorbent dosage on the adsorption process

In experiments to investigate the effect of adsorbent dosage on the adsorption process, the adsorbent dosages were determined as 1, 2, 3, 4 and 5 g L⁻¹. The particle size was set to 0.045–0.18 mm with initial Cu(II) concentration of 20 mg L⁻¹, and studies were completed at pH 5, stirring speed 300 rpm and temperature 20 °C. Results are shown in Fig. 1e.

When Fig. 1e is investigated, removal efficiency was calculated as 27.23% when initial adsorbent dosage was set to 1 g L⁻¹, while removal efficiencies were 57.69%, 73.34% and 77.07% for adsorbent dosages of 2, 3 and 4 g L⁻¹. At the final adsorbent dosage of 5 g L⁻¹, the removal efficiency reached maximum value compared to other studied adsorbent dosages and was calculated as 83.63%. The increase in adsorption removal efficiency as adsorbent dosage increased is thought to be due to the increase in adsorbent surface and pore volume available for the adsorption process (Dundar et al. 2008; Malkoc and Nuhoglu 2010). In the studies where the effect of adsorbent dosage was examined, the removal efficiencies and adsorption capacities were calculated as 83.63%, 77.07%, 73.34% and 7.23 mg g⁻¹, 7.88 mg g⁻¹, 7.46 mg g⁻¹ at 5 g L⁻¹, 4 g L⁻¹ and 3 g L⁻¹, respectively. As a result of variance analysis according to factorial trial pattern, it was determined that there was a difference between the groups ($p < 0.05$), and as a result of the variance analysis, it was statistically determined that the best removal efficiency was 5 g L⁻¹ dosage. However, the studies carried out in the next process where we examined the effect of different temperatures could not be carried out at adsorbent dosages of 5 g L⁻¹, 4 g L⁻¹ and 3 g L⁻¹. Because in these adsorbent dosages where the yields are high, Cu²⁺ removal efficiencies have reached to 100% at high temperatures, and in this case, the values obtained in temperature studies cannot be used to calculate the thermodynamic constants. The SSA adsorption capacity at 2 g L⁻¹ was calculated as 5.94 mg g⁻¹, so the decision was made to use adsorbent dosages of 2 g L⁻¹ for temperature experiments.



Effect of temperature on adsorption process

Experiments investigating the effect of temperature on the adsorption of Cu(II) ions using SSA were completed with particulate diameter 0.045–0.18 mm, at 300 rpm stirring speed and pH 5. Effects of different temperatures of 20, 30, 40 and 50 °C were investigated in studies with initial Cu(II) concentration and adsorbent dosage set to 20 mg L⁻¹ and 2 g L⁻¹. Data are shown in detail in Fig. 1f.

When Fig. 1f is investigated, the removal efficiency for Cu(II) at 20 °C was 57.69%, with removal efficiency rising by 4.17% to reach 61.86% at 30 °C. When temperature was increased to 40 °C, Cu(II) removal efficiency reached 67.29%, and finally at 50 °C, 72.55% Cu(II) removal efficiency was obtained. In addition to the removal efficiency, the adsorption capacity was also calculated as 7.53 mg g⁻¹ at 50 °C which they were the highest values and accepted as optimum value. Moreover, as a result of variance analysis according to factorial trial pattern, it was determined that there was a difference between the groups ($p < 0.05$), and as a result of the variance analysis, it was statistically determined that the best yield was at 50 °C. As can be clearly seen in Fig. 1f, the temperature parameter appears to be one of the most effective parameter on the adsorption of Cu(II) ions on SSA and removal efficiencies were increased with increasing temperatures (Malkoc and Nuhoglu 2010).

From the graphs given in Fig. 1, the effects of different parameters on adsorption of Cu(II) ions using sewage sludge ash (SSA) obtained from a wastewater sewage sludge thermal drying and incineration facility can be clearly observed. Adsorption equilibrium was reached in 10 min. The calculated maximum Cu(II) adsorption of 83.63% occurred at 20 °C, pH 5 and 300 rpm stirring speed, with initial Cu(II) ion concentration and adsorbent dosage values set to 20 mg L⁻¹ and 5 g L⁻¹. Additionally, the maximum adsorption efficiency was

calculated as 7.53 mg g⁻¹ when particulate size, pH, stirring speed, initial Cu(II) ion concentration, adsorbent dosage and temperature were set to 0.045–0.18 mm, 5, 300 rpm, 20 mg L⁻¹, 2 g L⁻¹ and 50 °C, respectively. Removal of Cu(II) ions with adsorbents in similar studies in the literature is given in Table 2.

Adsorption isotherm models

Adsorption capacity is determined with equilibrium adsorption isotherms defined by constants based on factors like the surface properties and affinity of the adsorbents. Using the experimental data obtained in our study, the four leading adsorption isotherm models of Langmuir, Freundlich, Dubinin–Radushkevich and Temkin were used and the results are shown in Fig. 2 and Table 3.

The simplest theoretical models for adsorption are the Langmuir, Freundlich, Dubinin–Radushkevich and Temkin models represented with Eqs. (1)–(4), respectively. When Fig. 2 and Table 3 are investigated in detail, the best fit among the four models was for the Langmuir isotherm with $R^2 = 0.9582$ compared to the other models.

$$\frac{1}{q_e} = \left(\frac{1}{a \cdot K_L} \right) \cdot \left(\frac{1}{C_e} \right) + \left(\frac{1}{a} \right); \quad R_L = \frac{1}{1 + K_L \cdot C_0} \quad (1)$$

$$\log q_e = \ln K_f + \frac{1}{n} \cdot \log C_e \quad (2)$$

$$\ln q_e = \ln q_s \cdot - K_{D-R} \cdot \epsilon^2; \quad E = \left[\frac{1}{\sqrt{2} \cdot B_{D-R}} \right] \text{ and } \epsilon = R \cdot T \cdot \ln \left[1 + \frac{1}{C_e} \right] \quad (3)$$

Table 2 Similar studies related to removal of Cu(II) ions with adsorbents

Adsorbent	q_m (mg g ⁻¹)	pH	References
Chitosan beads	64.62	4.5	Ngah and Fatinathan (2008)
Chitosan–GLA 1:1 ratio beads	31.20		
Chitosan–GLA 2:1 ratio beads	19.51		
Chitosan–alginate beads	67.66		
Cotton ball	11.40	5.0	Ozsoy and Kumbur (2006)
Dead fungal biomass (<i>P. pulmonarius</i>)	6.20	4.0	Veit et al. (2005)
Dead fungal biomass (<i>S. commune</i>)	1.52		
Sawdust	1.79	7.0	Yu et al. (2000)
Bagasse fly ash	2.26	4.0	Gupta and Ali (2000)
Peanut hulls	2.95	5.0	Ozsoy et al. (2007)
Wheat shell	8.34	5.0	Basci et al. (2004)
Tree fern	10.6	<6.0	Ho et al. (2002)
Sphagnum moss peat	12.4	5.0	Ho and McKay (2000)
Sewage sludge ash (SSA)	7.53	5.0	This study

Fig. 2 Adsorption isotherm models (particle size: 0.045–18 mm, pH: 5, stirring speed: 300 rpm, m : 2 g L⁻¹, T : 20 °C). **a** Langmuir adsorption isotherm for Cu(II) by SSA, **b** Freundlich adsorption isotherm for Cu(II) by SSA, **c** Dubinin–Radushkevich adsorption isotherm for Cu(II) by SSA, **d** Temkin adsorption isotherm for Cu(II) by SSA

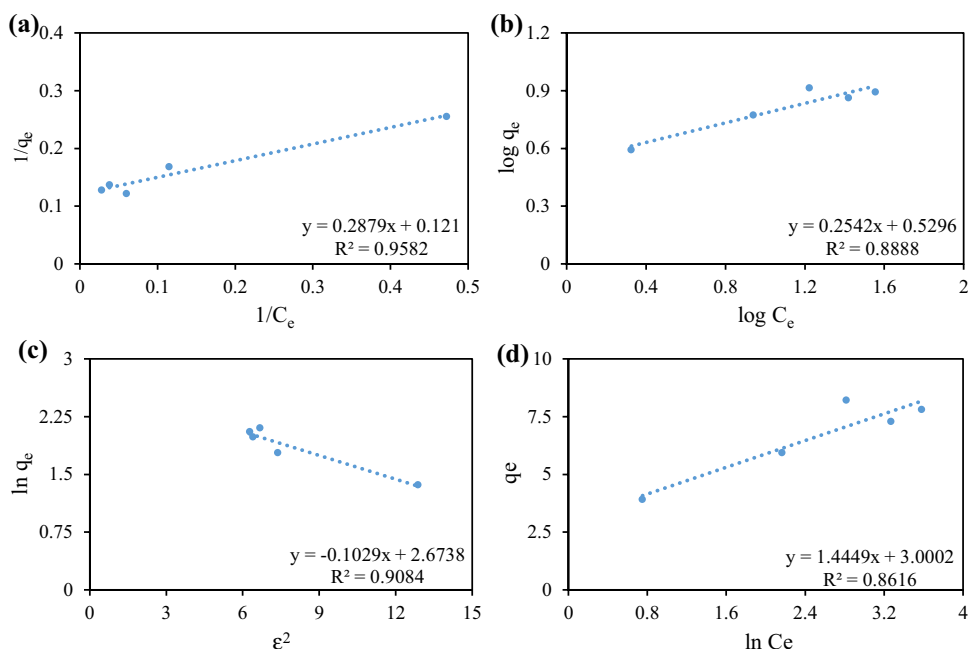


Table 3 Isotherm constants (particle size: 0.045–18 mm, pH: 5, stirring speed: 300 rpm, m : 2 g L⁻¹, T : 20 °C)

Isotherm constants	Values	Isotherm constant	Values
<i>Langmuir isotherm</i>		<i>Freundlich isotherm</i>	
a (mg g ⁻¹)	8.2645	n (L mg ⁻¹)	3.9339
K_L (L mg ⁻¹)	0.42	K_F (mg g ⁻¹)	3.3853
R^2	0.9582	R^2	0.8888
<i>Dubinin–Radushkevich isotherm</i>		<i>Temkin isotherm</i>	
q_s (mg g ⁻¹)	14.4949	B (j mol ⁻¹)	1.4449
K_{D-R} (mol ² KJ ²)	0.1029	K_T (L g ⁻¹)	7.9758
E (kJ mol ⁻¹)	2.2043	R^2	0.8616
R^2	0.9084		

$$q_e = \frac{R \cdot T}{b_T} \cdot \ln K_T + \frac{R \cdot T}{b_T} \cdot \ln K_e; \quad B = \frac{R \cdot T}{b_T} \quad (4)$$

Here, q_e is amount of adsorbate in the adsorbent at equilibrium (mg g⁻¹), C_e is adsorbate equilibrium concentration (mg L⁻¹), K_L is a constant related to net enthalpy of adsorption, a is the amount of adsorbed matter per unit weight of adsorbent forming a single layer on the surface (mg g⁻¹), R_L is related to the type of isotherms, K_F is the Freundlich adsorption constant (mg g⁻¹), n is the Freundlich adsorption constant (L mg⁻¹), q_s is theoretical isotherm saturation capacity (mg g⁻¹), K_{D-R} is Dubinin–Radushkevich isotherm constant (mol² kJ²), ϵ is Dubinin–Radushkevich isotherm constant, E is per molecule of adsorbate, B_{DR} is denoted as the isotherm constant, R represents the gas constant (8.314 J mol⁻¹ K⁻¹), K_T is the Temkin isotherm equilibrium binding constant (L g⁻¹), b_T is the Temkin constant related

to the heat of adsorption (J mol⁻¹), and T is the temperature (K).

The Langmuir isotherm assumes that adsorption occurs on a homogeneous surface and the number of active sites on the adsorbent is constant. According to the Langmuir isotherm, adsorption forms a single layer and maximum adsorption is adsorption at the moment when molecules bound to the adsorbent surface saturate the layer. The R_L values examine the types of isotherm: irreversible isotherm ($R_L = 0$), favorable isotherm ($0 < R_L < 1$), linear isotherm ($R_L = 1$) and unfavorable isotherm ($R_L > 1$) (Ucun 2011; Shafiee et al. 2020). The R_L values were found to be 0.1923, 0.1064, 0.0794, 0.0562 and 0.0455 when initial Cu(II) concentrations were 10, 20, 30, 40 and 50, respectively. All the R_L values obtained using Eq. (1) for Cu(II) adsorption were in the range of 0 to 1, and this shows that adsorption of Cu(II) onto the SSA is favorable.

Furthermore, the E (kJ mol⁻¹) value from the Dubinin–Radushkevich isotherm model is used to estimate the type of chemical or physical sorption process. If $1 < E$ (kJ mol⁻¹) < 8 , physical sorption becomes the dominant mechanism, and if $8 < E$ (kJ mol⁻¹) < 16 , the sorption reaction can be explained by a chemical sorption mechanism (Balarak et al. 2017).

Adsorption kinetics for Cu(II) ions

In light of data obtained from experiments completed at different temperatures, the pseudo-first-order and pseudo-second-order kinetic models given in Eqs. (5), and (6) were used for adsorption of Cu(II) ions by SSA. Data obtained using these equations are given in Fig. 3 and Table 4.

$$\ln(q_e - q_t) = \ln q_e - k_1 \cdot t \quad (5)$$

$$\frac{t}{q_t} = \frac{1}{k_2 q_e^2} + \frac{t}{q_e} \quad (6)$$

Here, q_t is amount of adsorbate in the adsorbent at time t (mg g^{-1}), k_1 is the rate constant of pseudo-first-order (mg L^{-1}), k_2 is the rate constant of pseudo-second-order ($\text{g mg}^{-1} \text{min}^{-1}$) and t is time.

The fit for the Cu(II) ion adsorption reaction on SSA to pseudo-first-order and pseudo-second-order kinetic equations is acceptable when values at or close to 1 are obtained from the R^2 values for the $\ln(q_e - q_t)$ against t graph and the t/q_t against t graph, respectively. Based on the results in Fig. 3 and Table 4, the adsorption of Cu(II) ions on SSA complies with the pseudo-second-order kinetic model. The q_e value calculated in the pseudo-second-order kinetic model

was found to be very close to the value obtained from experimental data.

Additionally, activation energy (E_a) defines the amount of energy required for a chemical reaction to occur. It can be defined as the amount of energy ensuring all molecules on a molar substrate are in transition and chemical adsorption occurs when the adsorption energy is 20–100 kcal mol^{-1} . Data obtained in experiments are shown in Fig. 4a, with activation energy calculated using Eq. (7).

$$\ln k_2 = \ln A - \frac{E_a}{R \cdot T} \quad (7)$$

The physisorption process normally has activation energy of 5–40 kJ mol^{-1} , while chemisorption has higher activation energy (40–800 kJ mol^{-1}) (Nollet et al. 2003; Wu 2007). With the values in Fig. 4a and with the aid of Eq. (7), the E_a value was calculated as 33.77 kcal mol^{-1} and the adsorption process can be said to occur chemically.

Fig. 3 Regression of kinetic plots at different temperature for adsorption of Cu(II) ions with SSA (particle size: 0.045–18 mm, pH: 5, stirring speed: 300 rpm, C_0 : 20 mg L^{-1} , m : 2 g L^{-1}). **a** Pseudo-first-order model, **b** pseudo-second-order model

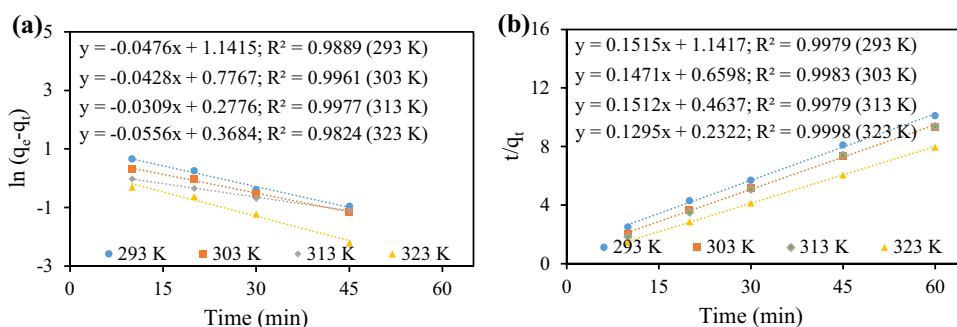
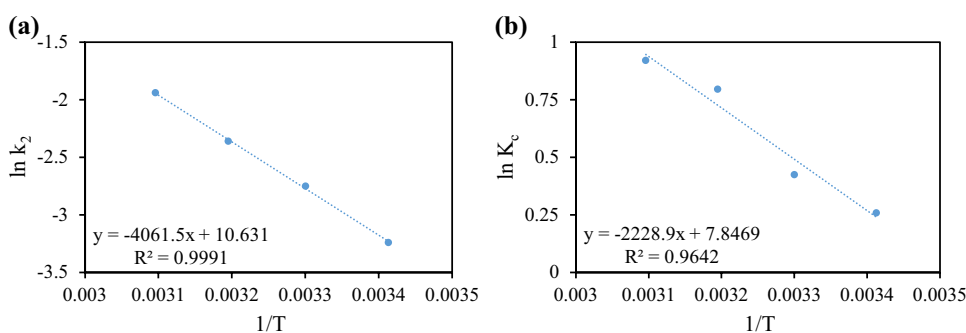


Table 4 Kinetic parameters for adsorption of Cu(II) ions with SSA (particle size: 0.045–18 mm, pH: 5, stirring speed: 300 rpm, C_0 : 20 mg L^{-1} , m : 2 g L^{-1})

T (K)	$q_{e,\text{exp}}$ (mg g^{-1})	Pseudo-first-order kinetic model			Pseudo-second-order kinetic model		
		k_1 (min^{-1})	$q_{e,\text{cal}}$ (mg g^{-1})	R^2	k_2 ($\text{g mg}^{-1} \text{min}^{-1}$)	$q_{e,\text{cal}}$ (mg g^{-1})	R^2
293	5.9385	0.0476	3.1315	0.9889	0.1503	1.7313	0.9985
303	6.4095	0.0428	2.1743	0.9961	0.1462	2.9895	0.9985
313	6.394	0.0309	1.3200	0.9977	0.1503	4.1771	0.9983
323	7.526	0.0556	1.4454	0.9824	0.1293	8.5985	0.9987

Fig. 4 Regressions for thermodynamic parameters (particle size: 0.045–18 mm, pH: 5, stirring speed: 300 rpm, C_0 : 20 mg L^{-1} , m : 2 g L^{-1}). **a** Arrhenius plot for adsorption of Cu(II) ions with SSA, **b** van't Hoff plot for adsorption of Cu(II) ions with SSA



Thermodynamic parameters

The enthalpy (ΔH°) and entropy (ΔS°) values are found by drawing the $\ln K_c$ against $1/T$ graph, and results are shown in Fig. 4b. Here, Gibbs free energy (ΔG°) values were found for every temperature with the aid of Eq. (8), while ΔH° and ΔS° values are calculated from the slope of the graph

– $\Delta H^\circ/R$ expressed in Eq. (9) and the intersection point of $\Delta S^\circ/R$. The results are given in Table 5.

$$\Delta G^\circ = -R \cdot T \cdot \ln K_c \quad (8)$$

$$\ln K_c = \frac{\Delta S^\circ}{R} - \frac{\Delta H^\circ}{R \cdot T} \quad (9)$$

where K_c is the equilibrium constant of adsorption.

Table 5 Thermodynamic parameters (particle size: 0.045–18 mm, pH: 5, stirring speed: 300 rpm, C_o : 20 mg L⁻¹, m : 2 g L⁻¹)

T (K)	ΔG° (kJ mol ⁻¹)	ΔH° (kJ mol ⁻¹)	ΔS° (kJ mol ⁻¹ K ⁻¹)
298	-0.6325	18.5311	0.0652
308	-1.0719		
318	-2.0724		
333	-2.4727		

Adsorption mechanism determined with SEM, FTIR and XRD analyses

The surface features of SSA before and after experiments were investigated using an SEM device, and the SEM microphotographs are shown in Fig. 5. When Fig. 5 is investigated, the surface morphology of SSA was different before

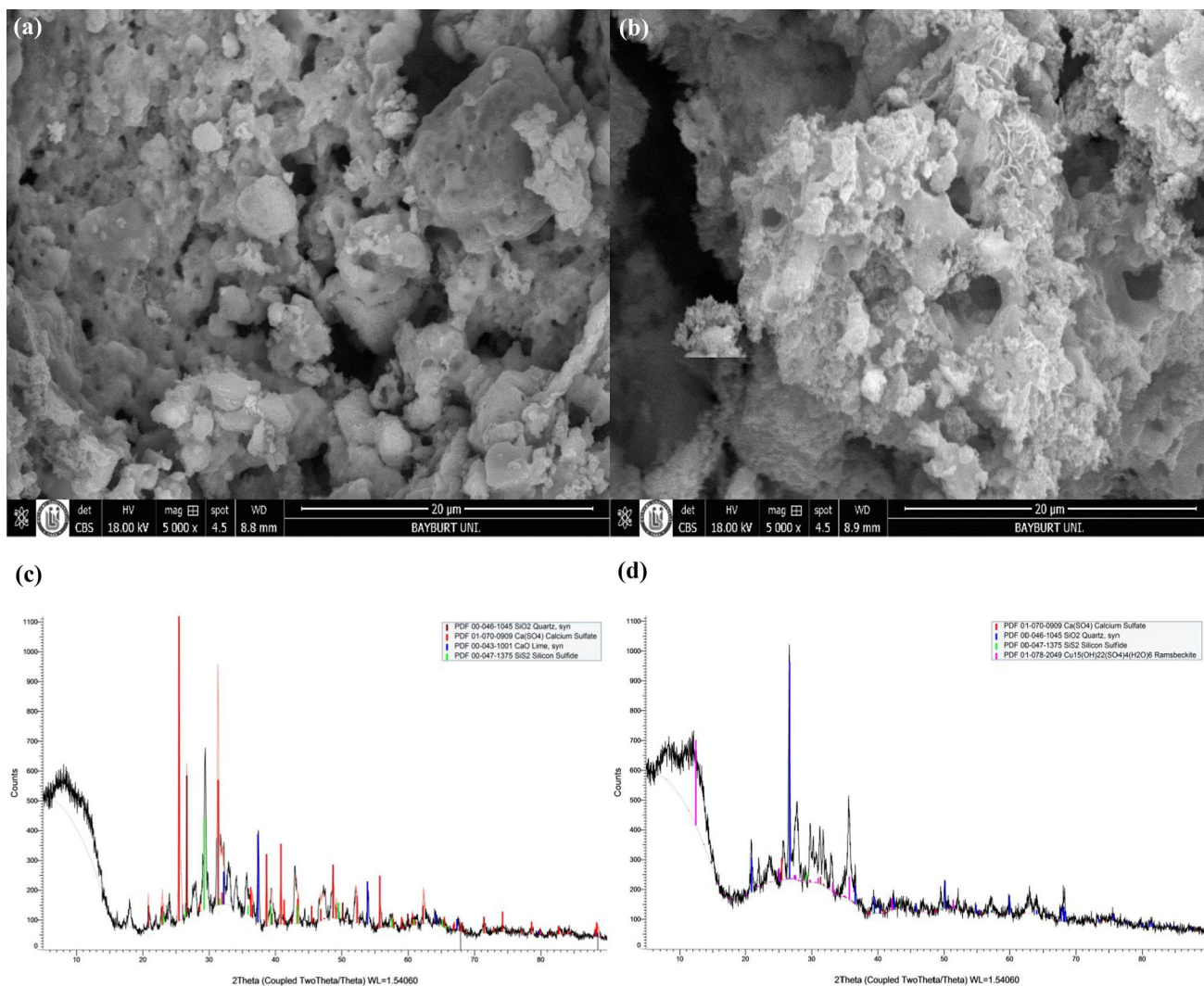


Fig. 5 SEM photomicrographs and XRD patterns of SSA. **a** SEM photomicrographs before adsorption, **b** SEM photomicrographs after adsorption, **c** XRD patterns before adsorption, **d** XRD patterns after adsorption



and after experiments. After the experiment, the surface of SSA was more irregular compared to before the experiments and Cu(II) can be seen chemically bound and/or physically adhered to the SSA surface (Feng et al. 2009).

FTIR analyses of SSA used a Fourier transform infrared spectrometry device in an attempt to characterize the bonds between molecules or compounds in the structure and functional groups. Data are given in Fig. 6 and Table 6.

When Table 6 is investigated, adsorption bands at 672 cm^{-1} , 873 cm^{-1} , 1099 cm^{-1} , 1403 cm^{-1} and 1618 cm^{-1}

belonging to Si–O, Si–O–Si, O–C–O and O–H bonds are observed with high intensity. Additionally, bands at 586, 571 and 1021 cm^{-1} participate weakly in the reaction and affect adsorption. The adsorption equilibrium was reached in a short duration of 10 min which is accepted as another marker that the very intense bands participated strongly in adsorption.

A Bruker D8 Discover XRD device was used to determine the structural features of SSA before and after the experiments and the data are shown in Fig. 5c, d. When

Fig. 6 FTIR spectra for SSA **a** before adsorption, **b** after adsorption

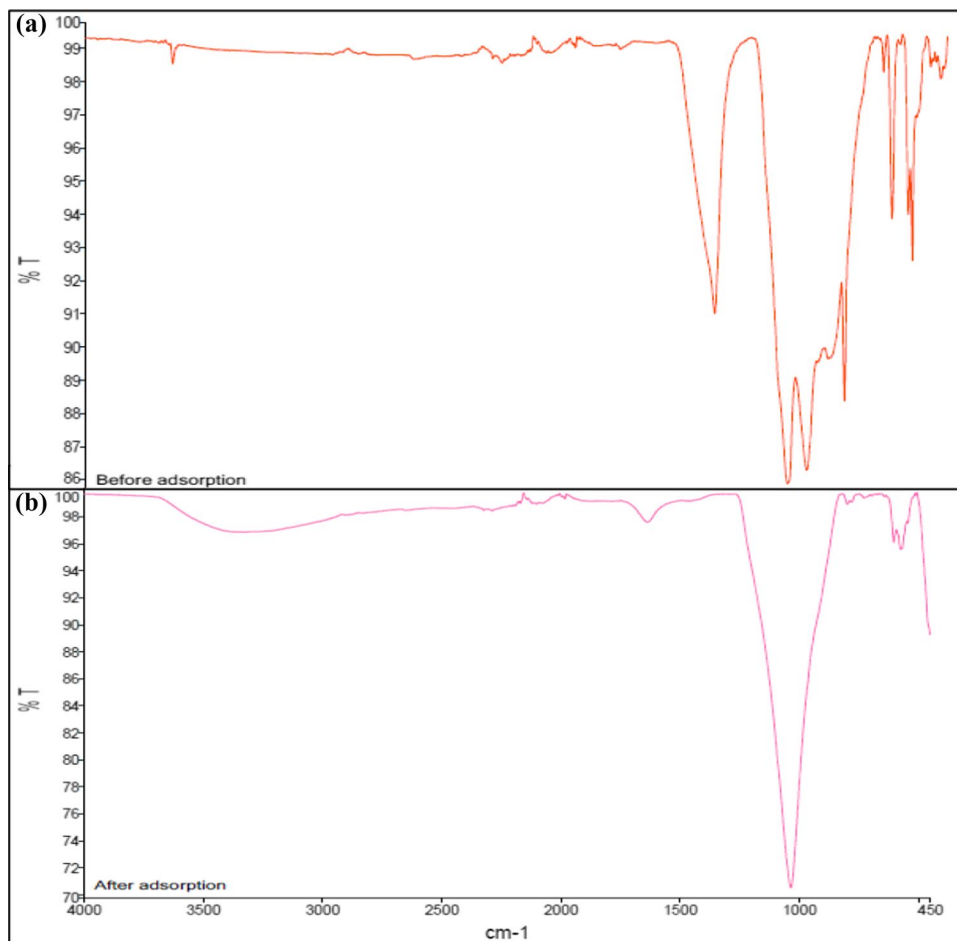


Table 6 FTIR spectral characteristics of SSA

IR peak	Assignments			
	Before adsorption	After adsorption	Differences	Functional groups
1	593	586	– 7	Fe–O bonds
2	609	571	– 38	Fe–O bonds
3	672	Disappear	Disappear	Si–O–Si bonds
4	873	Disappear	Disappear	Si–O or Si–O–Si bonds
5	1021	1028	+ 7	Si–O or Si–O–Si bonds
6	1099	Disappear	Disappear	Si–O or Si–O–Si bonds
7	1403	Disappear	Disappear	O–C–O bonds
8	Disappear	1618	Disappear	O–H bonds



Fig. 5c, d is investigated, though there is copper present in SSA before experiments, copper was adsorbed after the experiments. The $\text{Ca}(\text{SO}_4)$ compound observed in Fig. 5c is relatively reduced in Fig. 5d with $\text{Cu}_{15}(\text{OH})_{22}(\text{SO}_4)_4(\text{H}_2\text{O})_6$ identified on SSA after the experiments. This situation confirms the E_a value calculated with the aid of Eq. (7).

Conclusion

This research aimed to achieve heavy metal adsorption from wastewater using SSA, a pollutant material which is abundant, very cheap and has high metal-binding capacity. The adsorbent used in experiments was SSA obtained from GASKI Wastewater Sewage Sludge Thermal Drying and Incinerator Facility located in Gaziantep. SSA was concluded to be environmentally friendly and economic for the removal of Cu(II) ions. The following results were obtained in the study.

- Adsorption equilibrium was reached in almost 10 min.
- The effects of particulate size, pH, stirring speed, initial ion concentration, adsorbent dosage and temperature were investigated in order. Experiments completed under optimum conditions had Cu(II) removal efficiency of 83.63%.
- Calculations were performed using the Langmuir, Freundlich, Dubinin–Radushkevich and Temkin isotherm models, and the isotherm model with best fit was determined to be the Langmuir model.
- Adsorption kinetics abided by the pseudo-second-order model.
- Based on kinetic studies, the adsorption process was endothermic with maximum adsorption capacity of 7.53 mg g^{-1} .
- The results of thermodynamic research showed the adsorption reaction was spontaneous ($\Delta G^\circ < 0$), endothermic ($\Delta H^\circ > 0$) and reversible ($\Delta S^\circ > 0$ and close to zero).

SSA has great potential as a material produced at the end of a mandatory process; in other words, it is a heavy metal adsorbent without cost. In addition to being a cheap, effective and abundant potential adsorbent to treat wastewater containing Cu(II), regeneration is not required as it is waste.

Acknowledgements This research was supported by Bayburt University Scientific Research Projects (BAP) Coordination Unit within the scope of Project No: 2018/02-69001-05. Also, I owe a debt of gratitude to Prof. Dr. Yaşar Nuhoglu from Yıldız Technical University Department of Environmental Engineering, all the valued employees at Gaziantep Water and Sewerage Administration (GASKI) and all the valued employees at Atatürk University Department of Environmental Engineering and Laboratories.

References

- Abdullahi AA, Ighalo J, Ajala O, Ayika SO (2020) Physicochemical analysis and heavy metals remediation of pharmaceutical industry effluent using bentonite clay modified by H_2SO_4 and HCl. *J Turk Chem Soc Sect A Chem* 7(3):727–744
- Ahmad A, Rafatullah M, Sulaiman O, Ibrahim MH, Chii YY, Siddique BM (2009) Removal of Cu (II) and Pb (II) ions from aqueous solutions by adsorption on sawdust of Meranti wood. *Desalination* 247:636–646
- Akbal F, Camcı S (2011) Copper, chromium and nickel removal from metal plating wastewater by electrocoagulation. *Desalination* 269:214–222
- Aziz H, Othman N, Yusuff M, Basri D, Ashaari F, Adlan M, Othman F, Johari M, Perwira M (2001) Removal of copper from water using limestone filtration technique: determination of mechanism of removal. *Environ Int* 26:395–399
- Balarak D, Mostafapour FK, Azarpira H, Joghataei A (2017) Langmuir, Freundlich, Temkin and Dubinin–Radushkevich isotherms studies of equilibrium sorption of ampicillin onto montmorillonite nanoparticles. *J Pharm Res Int* 20(2):1–9
- Banerjee M, Kumar BR, Das SK (2019) Adsorptive removal of Cu (II) by pistachio shell: isotherm study, kinetic modelling and scale-up designing-continuous mode. *Environ Technol Innov* 15:100419
- Basci N, Kocadagistan E, Kocadagistan B (2004) Biosorption of copper (II) from aqueous solutions by wheat shell. *Desalination* 164:135–140
- Bereket G, Arog AZ, Özel MZ (1997) Removal of Pb (II), Cd (II), Cu (II), and Zn (II) from aqueous solutions by adsorption on bentonite. *J Colloid Interface Sci* 187:338–343
- Bingul Z, Gurbuz H, Aslan A, Ercisli S (2016) Biosorption of zinc (II) from aqueous solutions by nonliving lichen biomass of *Xanthoria parietina* (L.) Th. Fr. *Environ Eng Manag J* 15(12):2733–2740
- Chang Y-C, Chen D-H (2005) Preparation and adsorption properties of monodisperse chitosan-bound Fe_3O_4 magnetic nanoparticles for removal of Cu (II) ions. *J Colloid Interface Sci* 283:446–451
- Dundar M, Nuhoglu C, Nuhoglu Y (2008) Biosorption of Cu (II) ions onto the litter of natural trembling poplar forest. *J Hazard Mater* 151:86–95
- Escobar C, Soto-Salazar C, Toral MI (2006) Optimization of the electrocoagulation process for the removal of copper, lead and cadmium in natural waters and simulated wastewater. *J Environ Manag* 81:384–391
- Feng N, Guo X, Liang S (2009) Adsorption study of copper (II) by chemically modified orange peel. *J Hazard Mater* 164:1286–1292
- Gündoğan R, Acemioğlu B, Alma MH (2004) Copper (II) adsorption from aqueous solution by herbaceous peat. *J Colloid Interface Sci* 269:303–309
- Gupta VK, Ali I (2000) Utilisation of bagasse fly ash (a sugar industry waste) for the removal of copper and zinc from wastewater. *Sep Purif Technol* 18:131–140
- Gupta VK, Agarwal S, Bharti AK, Sadegh H (2017) Adsorption mechanism of functionalized multi-walled carbon nanotubes for advanced Cu (II) removal. *J Mol Liq* 230:667–673
- Ho Y-S, McKay G (2000) The kinetics of sorption of divalent metal ions onto sphagnum moss peat. *Water Res* 34:735–742
- Ho Y, Huang C, Huang H (2002) Equilibrium sorption isotherm for metal ions on tree fern. *Process Biochem* 37:1421–1430
- Kizilkaya B, Tekinay AA, Dilgin Y (2010) Adsorption and removal of Cu (II) ions from aqueous solution using pretreated fish bones. *Desalination* 264:37–47
- Kocherginsky N, Yang Q (2007) Big Carrousel mechanism of copper removal from ammoniacal wastewater through supported liquid membrane. *Sep Purif Technol* 54:104–116



- Kubilay Ş, Gürkan R, Savran A, Şahan T (2007) Removal of Cu (II), Zn (II) and Co (II) ions from aqueous solutions by adsorption onto natural bentonite. *Adsorption* 13:41–51
- Kul ZE, Nuhoğlu Y, Kul S, Nuhoğlu Ç, Torun FE (2016) Mechanism of heavy metal uptake by electron paramagnetic resonance and FTIR: enhanced manganese (II) removal onto waste acorn of *Quercus ithaburensis*. *Sep Sci Technol* 51(1):115–125
- Lee S (2006) Geochemistry and partitioning of trace metals in paddy soils affected by metal mine tailings in Korea. *Geoderma* 135:26–37
- Malkoc E, Nuhoglu Y (2010) Nickel (II) adsorption mechanism from aqueous solution by a new adsorbent—waste acorn of *Quercus ithaburensis*. *Environ Prog Sustain Energy* 29(3):297–306
- Mateen QS, Khan SU, Islam DT, Khan NA, Farooqi IH (2020) Copper (II) removal in a column reactor using electrocoagulation: parametric optimization by response surface methodology using central composite design. *Water Environ Res* 92(9):1350–1362
- Miretzky P, Cirelli AF (2010) Cr (VI) and Cr (III) removal from aqueous solution by raw and modified lignocellulosic materials: a review. *J Hazard Mater* 180(1–3):1–19
- Mohammadi T, Moheb A, Sadrzadeh M, Razmi A (2005) Modeling of metal ion removal from wastewater by electrodialysis. *Sep Purif Technol* 41:73–82
- Mojdehi AP, Chenar MP, Namvar-Mahboub M, Eftekhari M (2019) Development of PES/polyaniline-modified TiO₂ adsorptive membrane for copper removal. *Colloids Surf A Physicochem Eng Asp* 583:123931
- Ngah WW, Fatinathan S (2008) Adsorption of Cu (II) ions in aqueous solution using chitosan beads, chitosan–GLA beads and chitosan–alginate beads. *Chem Eng J* 143:62–72
- Nollet H, Roels M, Lutgen P, Van der Meeren P, Verstraete W (2003) Removal of PCBs from wastewater using fly ash. *Chemosphere* 53(6):655–665
- Nuhoğlu Y, Ekmekyapar Kul Z, Kul S, Nuhoğlu Ç, Ekmekyapar Torun F (2021) Pb (II) biosorption from the aqueous solutions by raw and modified tea factory waste (TFW). *Int J Environ Sci Technol* 1–12. <https://doi.org/10.1007/s13762-020-03038-8>
- Ozmen M, Can K, Arslan G, Tor A, Cengeloglu Y, Ersoz M (2010) Adsorption of Cu (II) from aqueous solution by using modified Fe₃O₄ magnetic nanoparticles. *Desalination* 254:162–169
- Ozsoy HD, Kumbur H (2006) Adsorption of Cu (II) ions on cotton ball. *J Hazard Mater* 136:911–916
- Ozsoy HD, Kumbur H, Ozer Z (2007) Adsorption of copper (II) ions to peanut hulls and *Pinus brutia* sawdust. *Int J Environ Pollut* 31:125
- Pan S-C, Lin C-C, Tseng D-H (2003) Reusing sewage sludge ash as adsorbent for copper removal from wastewater. *Resour Conserv Recycl* 39:79–90
- Pandey PK, Sharma R, Roy M, Pandey M (2007) Toxic mine drainage from Asia's biggest copper mine at Malanjkhand, India. *Environ Geochem Health* 29:237–248
- Potgieter J, Potgieter-Vermaak S, Kalibantonga P (2006) Heavy metals removal from solution by palygorskite clay. *Miner Eng* 19:463–470
- Qdais HA, Moussa H (2004) Removal of heavy metals from wastewater by membrane processes: a comparative study. *Desalination* 164:105–110
- Rodrigues Pires da Silva J, Merçon F, Guimarães Costa CM, Radoman Benjo D (2016) Application of reverse osmosis process associated with EDTA complexation for nickel and copper removal from wastewater. *Desalin Water Treat* 57:19466–19474
- Shafiee M, Abedi MA, Abbasizadeh S, Sheshdeh RK, Mousavi SE, Shohani S (2020) Effect of zeolite hydroxyl active site distribution on adsorption of Pb (II) and Ni (II) pollutants from water system by polymeric nanofibers. *Sep Sci Technol* 55(11):1994–2011
- Soltani H, Belmokhtar A, Zeggai FZ, Benyoucef A, Bousalem S, Bachari K (2019) Copper (II) removal from aqueous solutions by PANI-clay hybrid material: fabrication, characterization, adsorption and kinetics study. *J Inorg Organomet Polym Mater* 29(3):841–850
- Tong X-J, Li J-Y, Yuan J-H, Xu R-K (2011) Adsorption of Cu (II) by biochars generated from three crop straws. *Chem Eng J* 172:828–834
- Turan NG, Mesci B, Ozgonenel O (2011) The use of artificial neural networks (ANN) for modeling of adsorption of Cu (II) from industrial leachate by pumice. *Chem Eng J* 171:1091–1097
- Turan F, Karan S, Ergenler A (2020) Effect of heavy metals on toxicogenetic damage of European eels *Anguilla anguilla*. *Environ Sci Pollut Res* 27(30):38047–38055
- Ucun H (2011) Equilibrium, thermodynamic and kinetics of reactive black 5 biosorption on loquat (*Eriobotrya japonica*) seed. *Sci Res Essays* 6(19):4113–4124
- Ulfa SM, Chamidah N, Kurniawan A (2019) Adsorption of Cu (II) in aqueous solution by modified sawdust cellulose. *IOP Conf Ser Earth Environ Sci* 239(1):012008
- Uogintė I, Lujanienė G, Mažeika K (2019) Study of Cu (II), Co (II), Ni (II) and Pb (II) removal from aqueous solutions using magnetic Prussian blue nano-sorbent. *J Hazard Mater* 369:226–235
- Veit MT, Tavares CRG, Gomes-da-Costa SM, Guedes TA (2005) Adsorption isotherms of copper (II) for two species of dead fungi biomasses. *Process Biochem* 40:3303–3308
- Wu CH (2007) Adsorption of reactive dye onto carbon nanotubes: equilibrium, kinetics and thermodynamics. *J Hazard Mater* 144(1–2):93–100
- Yu B, Zhang Y, Shukla A, Shukla SS, Dorris KL (2000) The removal of heavy metal from aqueous solutions by sawdust adsorption—removal of copper. *J Hazard Mater* 80:33–42
- Zhang L-J, Tao H-C, Wei X-Y, Lei T, Li J-B, Wang A-J, Wu W-M (2012) Bioelectrochemical recovery of ammonia–copper (II) complexes from wastewater using a dual chamber microbial fuel cell. *Chemosphere* 89:1177–1182

